Modeling hydrate phase transitions using mean-field approaches

Atle Svandal

Dissertation for the degree philosophiae doctor (PhD)
at the University of Bergen

February 2006

Preface

This thesis has been produced as a part of the NFR project No.101204 "Carbon dioxide storage in hydrate reservoir". The main focus of this project was to investigate the potential of storing carbon dioxide in hydrate reservoirs. The combination of storing of a climate gas while simultaneously benefitting from the recovery of a valuable natural gas. This process of reformation of hydrate is theoretically possible due to the fact that carbon dioxide hydrate is significantly more stable than methane hydrate. The kinetics of hydrate reformation is the inner core of the dynamics of this exploitation scheme and the phase field theory was adopted to investigate the kinetics of the hydrate phase transitions. Hydrate growth from aqueous solutions has been studied for both carbon dioxide and methane. Due to the fact that the growth rate of carbon dioxide hydrate is significantly higher than methane hydrate, more attention has been given to the study of carbon dioxide hydrate. Single crystal growth and dissociation at different geometries has been studied, including anisotropic growth for the carbon dioxide hydrate.

An important part of this thesis has been to provide the thermodynamical properties that are needed as input for the phase field theory. Different approaches and corresponding different models has been used along the way and the thermodynamic model has evolved from the simple carbon dioxide hydrate - water system to a full three-component three-phase description of the water-carbon dioxide-methane system. This model will be a basis for a full phase field theory approach to model the kinetics of hydrate reformation.

The phase field simulations requires a lot of computation time. Some parts of my PhD work has therefore also been devoted to acquiring computers and the organization of these in a cluster for parallel processing.

Acknowledgments

This work has been funded by The Research Council of Norway through project 101204 and Conoco-Phillips.

First I like to thank Bjørn Kvamme for being my supervisor through this period. He is always full of ideas and has been a valuable source for comments and contributions for this thesis and the papers.

I have also had the pleasure of working with László Gránásy. The collaboration with him and his group in Hungary has been very fruitful. He has generously shared his experiences and work on the phase field theory as one of the leading experts in the world.

I have appreciated the collaboration with present and former members of the thermodynamic modeling group and other friends and colleagues at the Department of Physics and Technology. I would also like to thank the administrative and technical staff.

Finally I would like to apologize to all my friends for not having been very available the last couple of months, this especially goes for my dear Marianne.

List of Papers

Paper 1: The Influence of Diffusion on Hydrate Growth
Atle Svandal, Bjørn Kvamme, László Gránásy, Tamás Pusztai
Proceedings of the First International Conference on Diffusion in Solids and Liquids, DSL-2005, July 6-8, University of Aveiro, Portugal (p739-744) and Journal of Phase Equilibria and Diffusion, 26,5,(p534-538),2005

Paper 2: The Phase Field Theory Applied to CO_2 and CH_4 Hydrate
Atle Svandal, Bjørn Kvamme, László Gránásy, Tamás Pusztai, Trygve Buanes, Joakim Hove
Journal of Crystal Growth, 287,(p486-490),2006

Paper 3: Modelling the dissociation of carbon dioxide and methane hydrate using the Phase Field Theory
Atle Svandal, Bjørn Kvamme, László Gránásy, Tamás Pusztai
Lecture Series on Computer and Computational Sciences, Selected Papers from the International Conference on Computational Methods in Sciences and Engineering, ICCMSE-2005

Paper 4: Modelling the dissociation of carbon dioxide and methane hydrate using the Phase Field Theory
Atle Svandal, Bjørn Kvamme, László Gránásy, Tamás Pusztai
submitted to conference journals of ICCMSE-2005

Paper 5: Thermodynamic properties and phase transitions in the $H_2O/CO_2/CH_4$ system
Atle Svandal, Tatyana Kuznetsova, Bjørn Kvamme
to appear in Physical Chemistry Chemical Physics

Paper 6: A multi-scale approach to gas hydrate formation. I. Homogeneous nucleation and growth
György Tegze, Tamás Pusztai, Gyula Toth, László Gránásy, Atle Svandal, Tatyana Kuznetsova, Trygve Buanes, Tatyana Kuznetsova, Bjørn Kvamme
submitted to Journal of Chemical Physics

Paper 7: Computer Simulation of CO_2 Hydrate Growth
Trygve Buanes, Bjørn Kvamme, Atle Svandal
Journal of Crystal Growth, 287,(p491-494),2006

Paper 8: Two approaches for Modelling Hydrate Growth
Trygve Buanes, Bjørn Kvamme, Atle Svandal
Lecture Series on Computer and Computational Sciences, Selected Papers from the International Conference on Computational Methods in Sciences and Engineering, ICCMSE-2005

Paper 9: Two approaches for Modelling Hydrate Growth
Trygve Buanes, Bjørn Kvamme, Atle Svandal
submitted to conference journals of ICCMSE-2005

Paper 10: Hydrate Sealing Effects related to storage of CO_2 in cold reservoirs
Bjørn Kvamme, László Gránásy, Tatyana Kuznetsova, Atle Svandal, Trygve Buanes
to appear in the Proceedings from the 7^{th} International Conference on Greenhouse Gas Control Technologies(GHGT-7), September 5-9, 2004, Vancouver, BC, Canada, paper no 257,(p1811-1815)

Paper 11: Phase field approaches to the kinetic modeling of hydrate phase transitions
Bjørn Kvamme, Atle Svandal, Trygve Buanes, Tatyana Kuznetsova, László Gránásy
Invited and reviewed chapter in a book related to AAPG. Hedberg Research Conference Natural Gas Hydrates: Energy Resource Potential and Associated Geologic Hazards, September 12-16, 2004, Vancouver, BC, Canada, submitted October 2005.

Paper 12: Flux of CO_2 through hydrate sealing of CO_2
Atle Svandal, Bjørn Kvamme
extended abstract submitted to the 8^{th} International Conference on Greenhouse Gas Control Technologies(GHGT-8), 2006

Contents

Chapter 1

Introduction

When I started my PhD in February 2003 I had never heard about the substance called hydrates. From this I find it natural to start out by explaining what gas hydrates really are. In section 1.1 I present a brief review of the most common hydrates, what they look like and what their most important properties are. Special attention is given to hydrate structure I which is the most relevant to the rest of the thesis. Next, in section 1.2 a brief review of the history of hydrates and the milestones that have led to the current interest in hydrates are given. The scope of this thesis is on the kinetics of hydrate phase transitions. Section 1.3 gives an introduction to the subsequent chapters by presenting the existing models and hypothesis on hydrate kinetics prior to this work. The background material to this chapter have been found in the books by Sloan [1] and Makogon [2]. These books give a much wider introduction to hydrates and its history than presented here. Other resources conferred are the original hydrate paper by van der Waals and Plateuw [3] and the doctoral thesis by Førrisdahl [4].

1.1 The structure of hydrate and its properties

Macroscopically hydrates look very similar to ice or snow, and they also have many similar properties. Microscopically the hydrate structure consists of water molecules forming a host lattice that is by itself thermodynamically unstable, but is stabilized by the inclusion of a second component. The second component, often referred to as the guest, can in general be any molecule provided that it is neither too large or too small to fit into the cavities that is formed by the water lattice structure. That is, unless the stabilizing molecule has some specific interaction with the water molecules. Molecules that may be captured inside the cavities includes O_2, N_2, CO_2, CH_4, HCl, SO_2 and even the noble gases A, Kr and Xe.

Hydrates are known to form at least three different structures denoted sI, sII and sH. The kind of structure depends on the size of the guest molecule. The structures differ in the composition and types of cavities that constitutes the hydrate structure. The scope of this work is on hydrates with carbon dioxide (CO_2) and/or methane (CH_4) as guests. These two components both form the structure I hydrate and special focus will therefore be on this specific structure. Hydrate structure I is normally formed with molecules smaller than 6Å, such

as CH_4 and CO_2. Structure II and structure H contains larger cavities and are formed from larger molecules, such as propane for sII and iso-pentane for sH. More information on these structures can be found in the book by Sloan [1].

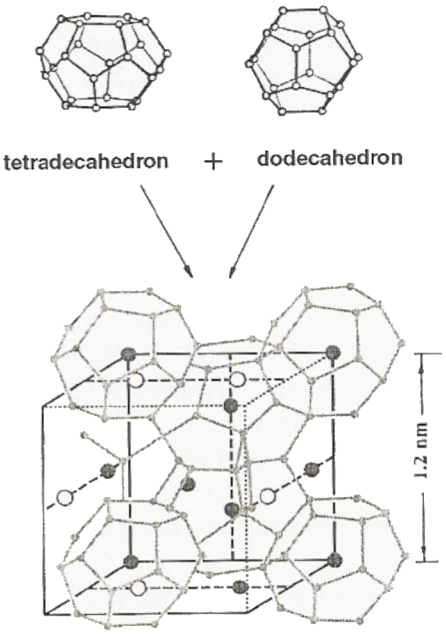

Figure 1.1: The unit cell of hydrate structure I, and the cavities constituting the structure. The figure is taken from the book of Makogon [2].

The unit cell of structure I shown in Fig. 1.1 contains 46 water molecules which enclose two different types of cavities. This is the smallest symmetric unit of this hydrate structure and a hydrate crystal of any size can be constructed by adding unit cells. The size of the unit cell is slightly dependent on temperature due to the temperature dependence of the hydrogen bonds [5]. At temperature $0°C$ the size of this unit cell is measured from crystallography to be 12.01Å(von Stackelberg and Muller[6].

The smaller cavities are each formed by a pentagonal dodecahedron with one water molecule at each of its 20 vertices. They are located at the center and at the vertices of the unit cell, giving an average of 2 small cavities per unit cell. The remaining 6 molecules form bridges between the smaller cavities in such a way that a second type of cavity is formed, a tetradecahedron, having two opposite hexagonal faces and 12 pentagonal faces adding up to 24 water molecules per cavity. There are 6 of these larger cavities per unit cell giving a small to large cavity ratio of 1 : 3. The smaller cavities are close to spherical and the average distance from the oxygen molecules in the water to the centers of the cages are 3.95Å. The larger cavities are slightly oblate and the distance from the oxygen to the center of cavity varies between 4.04Åand 4.65Å. If all the cavities were occupied by guest molecules the mole percent of water would be about 85%. Normally when hydrate forms, some of the cavitis will be left

empty, so the actual mole per cent water will be even larger than this. With such a high water content the properties of hydrates are assumed to depend very little on the guest molecules, other than to determine which structure hydrate will form. Based on the similarties in the water crystal structure one would also expect variations in properties between different hydrate structures to be less than the variation between hydrates and ice. The most striking property of hydrates is that they can be formed at temperatures higher than 0°C. The phase transition point also depends considerably on the pressure. The freezing temperature of ice on the other hand varies very little with pressure, and in the opposite direction of hydrate. When ice is put under pressure, for instance from an ice skate, the melting point is decreased and the ice may melt. When skating on ice this process together with the friction work melts the ice below the skates, creating a water film that reduces the friction between the metal and the ice. Hydrates become only more stable when exerted to pressure, so going skating on hydrates would be a different kind of experience. When ice freezes the specific volume of water increases by 9% which is considered abnormally high. Hydrates have an even larger expansion and increases 26-32% during the phase transition, if we only consider the water molecules. The thermal expansion of ice and hydrate sII is about the same while it is some 40% larger for structure I. Thermal conductivity is 5 times larger in ice than hydrates.

1.2 The history of hydrates

The first discovery of hydrates was either done by the English philosopher and naturalist Joseph Priestly in 1778 or by Sir Humphrey Davy in 1810. There are some uncertainty to whether Priestley's experiments with vitriolic air (SO_2) at a temperature below the water freezing point were observations of ice or hydrate. Davy's experiments with chlorine (Cl_2) were done at temperatures above the freezing point making this at least the first discovery of "warm ice". Neither of the experiments did attract much enthusiasm among scientists or industrialists at the time. From 1810 and the next one and a quarter of a century hydrate remained only of academic interest as a laboratory curiosity. The major goals for the research was to establish which compounds were able to form hydrates and to quantitatively describe the composition of the compounds in terms of how many water molecules were bound to each guest. During this time oil and gas became an important energy source. When large gas pipelines were constructed and put into operation in the USA in the 1920s the problem of plugs emerged in the transportation pipes during cold periods. These plugs were misinterpreted as solid ice formed from water remaining in the pipelines after construction. It was the American chemist E.G. Hammerschmidt who first identified the problem as hydrate plugging in 1934. This discovery is a milestone marking the beginning of the modern research era. From that time and until now a substantial amount of efforts have been invested into the challenges of being able to predict and prevent hydrate formation in pipelines and equipment during processing or transport. Much of the important historic research related to industrial problems are connected with D. Katz and R. Kobayashi, who devoted all their lives to hydrates. This long lived collaboration gave rise to new research techniques and technology, and many of the leading hydrate scientists in North America today is former students of these pioneers. In 1949 the group of

German scientist von Stackelberg reported two decades of X-ray hydrate crystal diffraction experiments leading to the determination of the two hydrate crystal structures sI and sII. A statistical theory for hydrates based on its structure were first proposed by van der Waals and Platteeuw in 1959.

Another special milestone in the history of hydrates was the discovery of natural gas hydrates in permafrost regions by a group of Russian researchers led by Makogon in 1967. The energy related to natural worldwide resources of methane in the form of hydrate has been estimated to twice the amount of the combined fossil fuel energy reserve. With the ever increasing demand for energy it is likely that the hydrate energy source will also be exploited in the near future provided that economically feasible technology becomes available. An interesting challenge in this respect is related to the fact that CO_2 hydrate is thermodynamically more stable than CH_4 hydrate. Theoretically this gives an opportunity for a win-win situation by injecting CO_2 into hydrate reservoirs and thus provide long term storage of CO_2 in the form of hydrate while releasing the original in situ natural gas. As a greenhouse gas methane is in the order of 25 times more aggressive than carbon dioxide per molecule. The wast amount of geological methane hydrate therefore also represents an environmental threat if it is dissociating and leaking into the atmosphere. It has been proposed that climate changes in the past may have been caused by methane hydrates contributing to an exponential growing feedback loop for global warming.

The fact that ions are unable to enter the hydrate structure (since the hydrogen bond network would collapse) is actually being used in desalination of water by means of hydrate. This is accomplished by means of a non-poisonous hydrate former, for instance CO_2, that readily forms hydrate and can easily be removed after dissociation of the hydrate. Storing natural gas in the form of hydrate has been proposed for transportation as an alternative to LNG(Liquid Natural Gas). The hydrate phase may also be used in refrigerators. These are just a few examples of many potential technical applications of the hydrate phase. Hydrate as a potential energy source, the environmental concern, the potential geohazard and a platform for technological developments represents a turn of the focus from hydrate as a purely industrial problem. Another aspect of CO_2 hydrate is related to aquifer storage of CO_2. Some regions, like for instance outside the north of Norway, the sea floor temperature may approach temperatures below 0°C. Storage of CO_2 in reservoirs in these regions may lead to hydrate formation at the interface between rising CO_2 plumes and the ground water for depths which corresponds to hydrate stability with respect to pressure and temperature.

With the development of the statistical model of van der Waals and Platteeuw [3], subsequent further developments of this model, and the adoption of this model into the industrial modeling tools, the hydrate community seem to have accepted this as an acceptable and usable state of the art equilibrium thermodynamics. The focus has therefore shifted towards the kinetics of hydrate phase transitions. The fundamental microscopic mechanisms behind the initial hydrate formation is still to a large extent an unanswered question. With the increasing interest in hydrate as an energy source as well as for technological applications a kinetic model of hydrate formation may be possible in the near future.

1.3 Kinetics of hydrate formation

Clusters of molecules need to grow to a certain size before they are thermodynamically stable, referred to as the critical size. Before achieving the critical size they may either grow or shrink. When the cluster reaches the critical size it will grow monotonically if it is not disturbed by competing clusters that are in a state of lower free energy. Hydrate formation are generally divided into these two parts, the process of initial nucleation, and the steady macroscopic growth. The time from the system is brought into a condition of supersaturation and until solid formation is observed is called the induction time or lag time. This does not mean that there is no hydrate present during this lag time. It could simply imply that initial hydrate sizes below visible range is slowing down transport of the hydrate building blocks across a heterogeneous system where the hydrate formers are in one phase and the aqueous phase are on the other side of the solid hydrate. Nucleation can either happen somewhere inside the bulk of a pure solution. This is denoted as homogeneous nucleation because all hydrate components are extracted from the same phase. Heterogeneous nucleation on the other hand, is a situation where the different components enter the hydrate from different phases. Nucleation on the interface between hydrate former phases, for instance a gas mixture and liquid water or ice, is a heterogeneous nucleation. In the open literature there are also experimental observations that have been discussed in terms of homogeneous nucleation while there exist photographic evidence that they most likely are heterogeneous because the dissolved hydrate formers has adsorbed onto a metal surface or other surfaces. The guest molecules are therefore extracted from an adsorbed phase while the water is taken from the solution and the nucleation is, by definition, heterogeneous. Homogeneous nucleation of hydrates are considered an anomaly with heterogeneous nucleation occurring much more frequently. The Gibbs free energy (ΔG) difference between a small solid particle and the solution can be expressed in terms of the surface free energy (ΔG_s) and the volume free energy (ΔG_v).

$$\begin{aligned} \Delta G &= \Delta G_s + \Delta G_v \\ &= 4\pi r^2 \sigma + \frac{4}{3}\pi r^3 \Delta g_v \end{aligned} \tag{1.1}$$

Here (Δg_v) is the free energy change per unit volume and σ is the interfacial tension. The surface gives a positive contribution to the free energy while the free energy change from liquid to solid is negative. Adding the surface and volume contribution gives a maximum value for (ΔG) at a specific radius which corresponds to the critical size. Below the critical radius there is a free energy penalty in getting larger so the crystals will fluctuate by either growing or redissolving. The critical radius represents the minimum size for which a nucleus will only grow. A foreign particle or surface may reduce the critical radius and are therefore more likely to occur. The process of hydrate nucleation contains physical elements that gives rise to stochastic behavior. If we picture the system on a molecular level it is quite obvious that the balance between movement and interactions, and corresponding probabilities for many-body interactions leading to clustering can give rise to many different scenarios. In the macroscopic experimental world within the notation of induction time as the onset of significant growth, it is very hard to determine this time at low driving forces. At higher driving forces the system is less stochastic and more predictable (macroscopi-

cally speaking). In addition to the thermodynamically conditions for nucleation the history of the water has also been shown to influence the induction time. It is believed that when ice or hydrate are dissociated a substantial amount of the the water structure remains. When the temperature is decreased for a second time the observed induction times are considerably shorter. Many experimental results imply some apparatus dependence making it not so easy to deduce any general conclusions.

Hydrate formation is normally observed to occur at the vapor-water interface or at the surface of the container. As mentioned in section 1.1 the hydrate guest composition may be as high as 15%. The solubility of guest molecules in water is normally very low suggesting that formation of hydrate in bulk phases are not very likely. Concentrations close to the 15% in hydrate can be found at the vapour-water interface and at the surface of the container through adsorption of guest molecules to the container walls, making these sites more likely for nucleation. Since hydrate nucleation normally occurs at the vapor-water interface this has also been the basis for molecular models. There is to date only a few hypotheses that attempts to describe the nucleation of hydrate at a molecular level.

Christiansen and Sloan [7] proposed a hypotheses following the classical nucleation theory. Water molecules are here assumed to form clusters around dissolved guest molecules. These clusters then combine to form unit cells, and when the size of agglomerated clusters reaches a critical size, growth begins. Another hypotheses has been proposed by Kvamme [8]. Gas molecules are here assumed to travel to a suitable site at the vapor-water interface where the water molecules form first partial, and then complete cages around the adsorbed species. Clusters join and grow on the vapor side of the surface until critical size is achieved. There are very limited experimental verification of these hypothesis so they should only be considered as conceptual aids in the understanding of the nucleation process.

In the growth phase mass and heat transfer become of major importance. Especially in growth from aqueous solutions, where the solubility is much less than hydrate concentrations, the mass transfer becomes important and may dominate the process. Two major models for hydrate growth exist, the work by Englezos et. al. [9] and the modified Englezos model by Skovborg and Rasmussen [10]. In general the change in the rate of crystal growth is expressed in terms of

$$\frac{dm}{dt} = KA(c - c^{eq}). \tag{1.2}$$

A is the crystal surface area, c and c^{eq} are the supersaturated and equilibrium concentration respectively. K is an overall transfer coefficient expressed in terms of diffusion and reaction coefficients k_d and k_r as

$$\frac{1}{K} = \frac{1}{k_d} + \frac{1}{k_r} \tag{1.3}$$

The concentrations in equation 1.2 are sometimes replaced by fugacities as in the Englezos model. To make this replacement one has to assume ideal liquid solutions, conservation of mass and constant temperature and pressure. By observing some restrictions and limitations in the Englezos model, Rasmussen and Skovborg were able to simplify the model. They assumed the process could be modeled as a mass transfer restriction through a liquid film at the gas-liquid

interface and reduced the number of differential equations from 5 to a single equation. These two models has yet only been shown to fit the data on which its parameters were based.

Chapter 2

The Phase Field Theory

In this chapter an introduction to the phase field theory is given. The most basic equations and concepts are presented in section 2.1. This model follows the formulation of Wheeler et. al.[11], which historically has been mostly applied to the descriptions of the isothermal phase transition between ideal binary-alloy liquid and solid phases. Section 2.2 deals with how the model can be extended to take into account anisotropy, polycrystalline growth and temperature dependence. In section 2.3 we discuss the properties of the hydrate systems relative to the phase field model. **Paper 6** gives a more extensive presentation of the phase field theory relative to hydrate growth and nucleation.

2.1 The governing equations

We consider an isothermal solution of two different components A and B which may exist in two different phases, solid and liquid, contained in a fixed region Ω. For the hydrate system the component A is water and component B is some guest molecule. Within the scope of this work B is then CO_2 or CH_4. The solid state is represented by the hydrate and an aqueous solution represent the liquid phase. The solidification of the new solid phase is described in terms of the scalar phase field $\phi(x,t)$ and the local solute concentration of component B denoted by $c(x,t)$. The field ϕ is a structural order parameter assuming the values $\phi = 0$ in the solid and $\phi = 1$ in the liquid. Intermediate values correspond to the interface between the two phases. The starting point of the model is a free energy functional,

$$F = \int d^3x \left(\frac{\varepsilon_\phi^2 T}{2} |\nabla \phi|^2 + f(\phi, c) \right), \tag{2.1}$$

which is an integration over the system volume of the free energy density $f(\phi, c)$ and a gradient term correction to ensure a higher free energy at the interface between phases. For some notes on functionals see appendix A. The free energy density is given by

$$f(\phi, c) = WTg(\phi) + (1 - p(\phi))\, g_S + p(\phi) g_L \tag{2.2}$$

The phase field switches on and off the solid and liquid contributions g_S and g_L through the function $p(\phi) = \phi^3(10 - 15\phi + 6\phi^2)$, we note that $p(0) = 0$

and $p(1) = 1$. The binary alloys are normally treated as ideal solutions. The thermodynamics for the hydrate system is treated more rigorously and the free energy densities are presented in chapter 3. The quartic function $g(\phi) = \phi^2(1-\phi)^2/4$ ensures a double well form of the $f(\phi, c)$ with a free energy scale $W = (1-c)W_A + cW_B$, with $g(0) = g(1) = 0$. In the phase field literature the concentration c is the mole fraction of component B, $c = n_B/(n_A + n_B)$, i.e. the fraction of component B to the total. With the assumption that the molar volume is constant the mole fraction concentration and the volume concentration are related by $c_m = c_v \nu_m$, where ν_m is the average molar volume. In chapter 3 the term x will be used for the mole fraction, but following the phase field formulation c will be used here.

In order to derive a kinetic model we assume that the system evolves in time so that its total free energy decreases monotonically. Given that the phase field is not a conserved quantity, the simplest form for the evolution that ensures a minimization of the free energy is

$$\dot{\phi} = -M_\phi \frac{\delta F}{\delta \phi}, \tag{2.3}$$

with $M_\phi > 0$. We may also allow M_ϕ to depend on composition writing $M_\phi = (1-c)M^A + cM^B$. For the conserved quantity we may associate a flux to the concentration by writing

$$\dot{c} = -\nabla \cdot J_c. \tag{2.4}$$

Following classical linear irreversible thermodynamics we assume that near equilibrium the flow is linearly proportional to the force that drives it. We then write

$$J_c = -M_c \nabla \frac{\delta F}{\delta c}. \tag{2.5}$$

Putting 2.5 into 2.4 gives

$$\dot{c} = \nabla \cdot \left(M_c \nabla \frac{\delta F}{\delta c} \right). \tag{2.6}$$

In order to reproduce the Fick's law of diffusion in the bulk phases we chose $M_c = c(1-c)\frac{\nu_m}{RT} D$. Here D is the diffusion coefficient that in order to allow for different diffusivities in the solid and liquid can be expressed in terms of the respective diffusivity coefficient governed by the phase field as $D = D_S + p(\phi)(D_L - D_S)$. Now using the form of the free energy as in Eq. 2.1 the governing equations can be written as

$$\dot{\phi} = M_\phi \left(\varepsilon_\phi^2 T \nabla^2 \phi - WTg'(\phi) - p'(\phi)\left(g_L - g_S\right) \right) \tag{2.7}$$

and

$$\dot{c} = \tag{2.8}$$
$$\nabla \cdot \left(\frac{\nu_m}{RT} Dc(1-c) \nabla \left(\left(W_A - W_B\right) Tg(\phi) + \left(1 - p(\phi)\right) \frac{\partial g_S}{\partial c} + p(\phi) \frac{\partial g_L}{\partial c} \right) \right).$$

The model parameters ε_ϕ, W_A, W_B, M^A and M^B can be related to measurable quantities, just as we related M_c to the diffusivity. Considering the equilibrium condition the parameters can be related to the interface energy $\sigma_{A,B}$, the temperature of melting $T_{A,B}$ and the interface thickness $\delta_{A,B}$.

2.2 Extended models

To include the flow of heat in the simulation an energy or thermal field are introduced as in the work by Conti [12, 13]. The energy field is a conserved quantity and the time derivative can be derived by associating a flux to the flow of energy and a driving force as in equation 2.4 and 2.6.

$$\begin{aligned} \dot{e} &= -\nabla \cdot J_c. \\ \dot{e} &= \nabla \cdot \left(M_e \nabla \frac{\delta F}{\delta e} \right). \end{aligned} \tag{2.9}$$

For hydrate growth from aqueous solutions where the solvent concentration is at most a couple of percent, the chemical diffusion is assumed to completely dominate the process as discussed in **paper 1**. Constant temperature are assumed for this system, and a thermal field has not been included in our models.

The governing equations are so far formulated spherically symmetric. To model dendritic growth some asymmetry has to be introduced to the model. This is typically accomplished(see for instance [14]) by making the ε_ϕ in equation 2.1 dependent on the orientation of the phase field as $\varepsilon = \bar{\varepsilon}\eta = \bar{\varepsilon}(1+\gamma_\varepsilon cos(k_\varepsilon \theta))$ where $\bar{\varepsilon}$, γ_ε and k_ε are constants, and $tan\theta = \phi_y/\phi_x$. To study the soft impingement of alloy polycrystals László Gránásy [15] introduced a non conservative orientation field θ which is random in the liquid and has a constant value between 0 and 1 in the crystal that determine crystal orientation in the laboratory frame. The grain boundary energy is then assumed to act in the solid proportional to $|\nabla\theta|$. This is realized by adding a term $M|\nabla\theta|$ to the g_S term in equation 2.2. The respective equation of motion related to the orientation field is

$$\dot{\theta} = -M_\theta \frac{\delta F}{\delta \theta} + \xi_\phi. \tag{2.10}$$

Here M_θ is the mobility associated with the orientation. In order to model nucleation uncorrelated noise may be added to the governing equations as the ξ_ϕ term in equation 2.10, noise terms can be added to equation 2.3 and 2.6 in a similar fashion. Adding noise to the concentration field can be difficult because of the restriction on conservation of mass. In his work Gránásy relates the anisotropy to the orientation field $\varepsilon = \bar{\varepsilon}(1+\gamma_\varepsilon cos(n\vartheta - 2\pi\theta)$ where $tan\vartheta = \phi_y/\phi_x$ with n-fold symmetry.

The most general expression for the total free energy would also include a gradient term of the concentration. The free energy functional in 2.1 would then be on the form

$$F = \int d^3x \left(\frac{\varepsilon_\phi^2 T}{2} |\nabla\phi|^2 + \frac{\varepsilon_c^2 T}{2} |\nabla|^2 + f(\phi, c) \right). \tag{2.11}$$

In the simulations the extra gradient term are introducing numerical instabilities. The time step has to be reduced a factor of 100 depending on the value of ε_c. This parameter can be related to the aqueous/fluid interface, this has only been done in a backward estimation of the interface thickness from the phase field simulations. Theε_c^2 has been estimated to be about 40 times larger than ε_ϕ^2. For simulations of the aqueous/hydrate, where the concentration varies from 0 to full filling of the hydrate at about 0.15, the gradient term are neglected in the calculations.

2.3 Simulations of hydrate systems

Classically the phase field theory, as formulated for phase transition kinetics, has mostly been applied to model alloy solidification. There are some very important differences between binary metals and the hydrate systems that we focus on in the modeling conducted in this work. The most apparent is the very low solubility of the solute, CO_2 or CH_4, in the solvent, water. The simplest scenario for growth is from an initial nucleus in a supersaturated homogeneous solution. To our knowledge there are presently no published phase-field models that deal with heterogeneous growth. This is a necessary element in hydrate kinetics where most of the natural hydrate phase transitions involve a heterogeneous situation which in varying degrees are coupled to a homogeneous situation. The implication is typically that a hydrate film almost closes the free transport of molecules across the hydrate layer. In this respect the term almost closing implies simply that the diffusivity of water molecules and hydrate formers across the hydrate film is reduced to at least three orders of magnitude [16] lower than the corresponding diffusivities in liquid solutions. The real number are probably even lower since the actual experiment for the verification of these numbers are related to a shrinking bubble of CO_2 consumed by hydrate. The mechanism for mass exchange in the experiments is hardly a diffusion process since the bubble shrinks and constantly breaks its hydrate film and correspondingly opens up for "snapshots" of a free mass exchange. In view of this it is important to understand the homogeneous as well as heterogeneous growth features of hydrates since an initial extreme reduction in mass transport through the hydrate film from heterogeneous growth will be followed by a continued growth from dissolved hydrate former in the aqueous phase. Theoretically there will

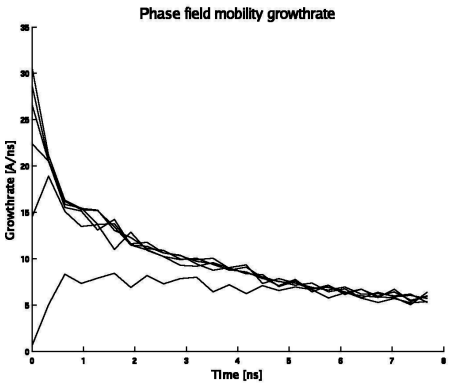

Figure 2.1: The growth rate at different values for the phase field mobility differing in range a factor 30.

be a corresponding continued growth from the water molecules dissolved in the hydrate former phase. In view of the small amount of water in this phase and the ratio of water to guests in the hydrate, this side of the further growth is not very important in the total situation. Compared to alloys the experimental data available for hydrate growth are few, especially at micro levels. Many different experimental techniques, like for instance stirring or macroscopic flow, are not

possible to include in the theoretical modeling. The experimental results are also known to include a lot of unknowns in terms of apparatus dependence on the results.

Our first simulations of the hydrate system was a parameter sensitivity study. The influence of a series of parameters on the growth rate were analyzed including the interface thickness, the interfacial free energy, the amplitude of noise, the phase field mobility, the orientation mobility and the spatial resolution. The results for the phase field mobility is shown in Fig. 2.1. The parameters in the study had little effect on the long time growth rate, but influenced the initial growth, and in some cases the critical size of the nuclei. From this study it became clear that for simulations with realistic model parameters, the dominating process was the mass transport. Further simulation results are presented in the papers and will not be repeated here.

Chapter 3

Thermodynamics of CO_2 and CH_4 hydrate

This chapter treats the development of the thermodynamical functions needed for the phase field simulations in chapter 2. Section 3.1 introduces some useful terms and relations that is later used in the development of the thermodynamic model. The free energies that goes into Eq. 2.2, i.e. g_S and g_L, can be calculated from the chemical potentials evaluated in section 3.2-3.4. Section 3.2 treats the general thermodynamics of the hydrate phase, while section 3.3 and 3.4 treats the fluid and aqueous thermodynamics respectively. In section 3.5 experimental data is compared to the predictions calculated from the thermodynamic model.

3.1 Thermodynamics and thermodynamic model systems

3.1.1 The Gibbs-Duhem Equation

One of the important general relations in thermodynamics is the Gibbs-Duhem equation. This relation shows that not all of the intensive variables T, p and μ_k are independent. It is obtained from the fundamental relation through which Gibbs introduced the chemical potential.

$$dU = TdS - pdV + \sum_k \mu_k dN_k \tag{3.1}$$

Assuming that the entropy is an extensive function of U, V, and N_k we have from the Euler theorem

$$U = TS - pV + \sum_k \mu_k N_k. \tag{3.2}$$

The general differential of this is

$$dU = Tds + SdT - Vdp + pdV + \sum_k (\mu_k dN_k + N_k d\mu_k) \tag{3.3}$$

The relation in 3.1 can only be consistent with 3.3 if the following relation holds:

$$SdT - VdP + \sum_k N_k d\mu_k = 0. \tag{3.4}$$

This relation is called the Gibbs-Duhem equation. In the case of constant temperature and pressure and with 2 components with mole fractions x_1 and x_2 it reduces to

$$x_1 d\mu_1 + x_2 d\mu_2 = 0. \tag{3.5}$$

3.1.2 The phase rule

When many components and more than two phases are in equilibrium, the chemical potential of all components should be the same in every phase it exists. Within a single phase the intensive variables temperature and pressure can in general be varied independently. However when we consider equilibrium situations between two phases we introduce constraints to the variables and they are no longer independent. A single phase can be characterized by $m + 2$ variables, in terms of pressure temperature and the chemical potential of m components in the system. The Gibbs-Duhem equation 3.4 places a restriction on these variables so there are only $m + 1$ independent variables, or we can say that a phase has $m + 1$ degrees of freedom. If each phase in a system is in internal equilibrium we have a total of $\pi(m + 1)$ independent variables, where π is the number of phases. If we assume that the entire system is in a state of internal equilibrium there are a total of $(\pi - 1)(m + 2)$ equilibrium relations that states that each component in all phases are in equilibrium. Then the number of independent variables, or number of degrees of freedom, is given by the number of intensive variables used to characterize the system minus the number of restrictions within it.

$$\begin{aligned} f &= \pi(m+1) - (\pi-1)(m+2) \\ &= m - \pi + 2 \end{aligned} \tag{3.6}$$

With two components (water and either CO_2 or CH_4) there will be two phases outside the hydrate stability region, the aqueous liquid phase and the fluid phase (CO_2 or CH_4). The number of degrees of freedom is 2, which means that the system is uniquely defined with respect to equilibrium when temperature and pressure is fixed. If the same system is brought into the hydrate stability region the number of possible phases increases to three and the number of degrees of freedom is reduced to 1. If the temperature is defined there will exist one unique pressure where all phases can exist in equilibrium. Correspondingly there will be a unique three phase equilibrium temperature if the pressure is defined. The most common situation in natural systems is that both pressure and temperature is defined and the system is thermodynamically overdetermined. In this case the system is not able to establish complete three phase equilibrium and the combination of the first and second laws of thermodynamics will dictate this system to approach a state of minimum free energy. Since the system is inside the hydrate stability zone this implies that hydrate is a more stable form of water than liquid water or ice and that the total free energy change over to hydrate represents a Gibbs free energy reduction. As a consequence the minimum free energy will dictate the asymptotic content of carbon dioxide or

methane dissolved in the aqueous solution to be those that represents a situation of equilibrium between the hydrate and the aqueous solution.

3.1.3 Residual thermodynamics

Thermodynamic deviations from the ideal gas behavior is denoted as residual thermodynamics and are indicated by a superscript R in the following. From the combined first and second law of thermodynamics and the ideal gas law we have for an ideal gas

$$d\mu_i = RTd\ln x_i P, \tag{3.7}$$

at constant temperature, where μ_i is the ideal gas chemical potential of component i with mole fraction x_i. To generalize this a new function f called the fugacity is introduced to obtain a general expression for the chemical potential of a component i.

$$d\mu_i = RTd\ln f_i \tag{3.8}$$

The fugacity can be interpreted as a corrected pressure. For a mixture of ideal gasses the fugacity equals the partial pressure $x_i P$ of the component, where x_i is the mole fraction. For convenience we also define the fugacity coefficient $\phi = f_i/(x_i P)$, which is the deviation factor from ideal gas partial pressure over to real fluid fugacity.

$$\ln\phi(T,P,\vec{x}) = \frac{\partial\left(\frac{NG^R}{RT}\right)_{T,P,N_{j\neq i}}}{\partial N_i} = \frac{\partial\left(\frac{NA^R}{RT}\right)_{T,V,N_{j\neq i}}}{\partial N_i} \tag{3.9}$$

The compressibility coefficient $Z = PV/RT$ and the corresponding equation for ideal gas can now be inserted into the Helmholtz free energy A or Gibbs free energy G depending on the form of the equation of state. The details of this can be found in any textbook on multicomponent thermodynamics and only the final results are repeated here.

$$\ln\phi(T,P,\vec{x}) = -\frac{1}{RT}\int_{\infty}^{\underline{V}}\left[\left(\frac{\partial P}{\partial N_i}\right)_{T,\underline{V},N_{j\neq i}} - \frac{RT}{\underline{V}}\right]d\underline{V} - \ln Z \tag{3.10}$$

The compressibility coefficient Z for the mixture is given by the specific equation of state used for the model calculations. In this work we have used the SRK equation of state [17]. Similarly the same equation of state is inserted for the pressure in the integrand and the resulting fugacity coefficient is an analytic expression of the SRK equation. See for instance [18] for the complete expression derived for this equation as well as some other commonly used equation of state. For a specific mixture with constant composition at a given temperature and pressure we also note that

$$\frac{G}{RT} = \sum_i x_i\frac{\mu_i^0(T,P)}{RT} + \sum_i x_i\ln x_i\phi_i(T,P,\vec{x}), \tag{3.11}$$

where μ_i^0 is the ideal gas chemical potential which can be calculated from the Helmholtz free energy using the actual molar volume which correspond to the specific condition of temperature and pressure. For this purpose methane is treated as an approximately spherical atom and the carbon dioxide molecule is

treated as a line with a specific angular momentum given by the bond lengths and masses. For every temperature, pressure and composition the molar volume and partial molar volumes of each component is calculated from the solution of the equation of state. The corresponding expression for the ideal gas chemical potential can be found in any textbook in physical chemistry.

3.1.4 Excess thermodynamics

An alternative formulation to the residual thermodynamics for liquid mixtures is the excess thermodynamics. In this formulation the reference state is the components as pure liquids at the system temperature and pressure. Parallel to the ideal gas in the residual formulation we now have an ideal liquid solution where all the components behave as if they were in a pure state. The chemical potential for an ideal solution can be expressed as

$$\mu_i = \mu_i^0 + RT \ln x_i \tag{3.12}$$

where μ_i^0 is the chemical potential of the pure liquid and x_i is the mole fraction. Deviations from this state is denoted the excess part and will be indicated by a E superscript in the following. To describe this deviation we introduce the activity a which is defined as the ratio f/f^0, and the activity coefficient which can be expressed in terms of the activity and the mole fraction as $\gamma_i = a_i/x_i$. The fugacity can then be expressed as $f = \gamma x f^0$, where f^0 is the ideal solution reference state. The specific change in the mixture properties due to the different cross-interactions between different molecules and all other non-ideal mixtures are incorporated in the excess stage expressed as

$$\mu_i^E = RT \ln \frac{x_i f_i^0 \gamma_i}{x_i f_i^0} = RT \ln \gamma_i \tag{3.13}$$

Equation 3.12 can now be extended with the excess term in Eq. 3.13 to give the chemical potential of a real liquid. The chemical potential of the pure components can be obtained in a number of fashions. In this work the residual chemical potential has been obtained through Molecular Dynamic simulations for state of the art simplified water models and corresponding ideal gas chemical potentials calculated according to straightforward statistical mechanics as briefly indicated under the discussion of residual thermodynamics. Another way to calculate the chemical potential of the pure component is with the aid of the saturation pressure $P^{sat}(T)$. At saturation pressure the gaseous and liquid phases are in equilibrium and the fugacities are the same. The liquid fugacity is then replaced by the gas fugacity and a simple integration over the pressure difference. The fugacity of pure liquid can then be expressed as

$$f_i^0 = \phi_i^{pure,gas}(T, P^{sat}) P^{sat} \exp\left(\int_{P^{sat}}^{P} \frac{\nu_w}{RT} dP \right) \tag{3.14}$$

where $\phi^{pure,gas}$ is the fugacity coefficient for pure gas and ν_w is the molar volume of liquid water. The limitation of this equation is that the actual components have a well defined saturation pressure. For supercritical components and ions which do not have a pure liquid reference state the most common is to use infinite dilution of the component in the solution as the reference state. An advantage of

this is that the chemical potential at infinite dilution can be estimated for model systems from molecular dynamics simulations. The ideal mixing term and the excess part will take the same form as in Eq. 3.12 and 3.13, but now the reference state is different so the asymptotic behavior of the activity coefficient will also be different. The pure liquid reference is termed the symmetric convention, where the activity coefficient $\gamma \to 1$ in the limit as $x \to 1$. In the asymmetric or unsymmetrical convention with infinite dilution as the reference state the activity coefficient $\gamma \to 1$ in the limit as $x \to 0$. The chemical potential can be written according to the asymmetric convention as

$$\mu_i = \mu_i^{\infty} + RT \ln x_i + RT \ln \gamma_i^{\infty} \tag{3.15}$$

Relative to the systems in this work CO_2 and CH_4 is treated according to the asymmetric convention while water in the aqueous solution is treated according to the symmetric convention. Activity coefficients as well as the chemical potentials at infinite dilution has in this work been estimated through fitting to experimental data as treated in section 3.3 and 3.4.

3.2 Hydrate Thermodynamics

The treatment of the hydrate thermodynamics is based on the extended adsorption theory by Kvamme and Tanaka [19]. The expression for chemical potential of water in hydrate is

$$\mu_w^H = \mu_w^{0,H} - \sum_j RT\nu_j \ln\left(1 + \sum_k h_{k_i}\right) \tag{3.16}$$

Here $\mu_w^{0,H}$ is the chemical potential for water in an empty hydrate structure and h_{k_i} is the cavity partition function of component k in cavity type j. The first sum is over cavity types, and the second sum is over components k going into cavity type j. Here ν_j is the number of type j cavities per water molecule. For hydrate structure I there are 3 large cavities and 1 small per 23 water molecules, $\nu_L = 3/23$ and $\nu_S = 1/23$. The chemical potential for the guest can be written as

$$\mu_k^H = \Delta g_{kj}^{inc} + RT \ln h_{k_j}, \tag{3.17}$$

where Δg_{kj}^{inc} is the free energy associated with the inclusion of guest molecule k in cavity j. In order to calculate the chemical potentials we have to relate the cavity partition function to the compositions. The relation between the filling fraction, the mole fractions and the cavity partition function is

$$\theta_{ki} = \frac{x_{ki}}{\nu_i(1 - x_T)} = \frac{h_{ki}}{1 + \sum_j h_{ki}}. \tag{3.18}$$

For a system with only one component occupying the large cavities, as is the case for CO_2 hydrate, the chemical potential of the guest molecule would reduce to

$$\mu_k^H = \Delta g_{kj}^{inc} + RT \ln\left(\frac{\theta_{kj}}{1 - \theta_{kj}}\right) \tag{3.19}$$

In the general case when both cavities are occupied by one or more components a more cumbersome approach is needed. For the multi-component system with

small cavities occupied my methane and large cavities occupied by both methane and carbon dioxide, we start out by assuming that the chemical potential of methane in the two cavities are the same. this gives a proportional relation between the two partition functions independent on composition.

$$\frac{h_{ml}}{h_{ms}} = e^{\beta(\Delta g^{inc}_{ms} - \Delta g^{inc}_{ml})} = A \tag{3.20}$$

The mole fraction of methane x_m is the sum of the mole fraction in each cavity, i.e. large x_{ml} and small x_{ms}. We express these mole fraction in terms of the cavity partition function from equation 3.18

$$\begin{aligned} x_{ms} + x_{ml} &= x_m \\ \frac{h_{ms}}{1+h_{ms}}\nu_s + \frac{h_{ml}}{1+h_{ml}+h_{cl}}\nu_l &= \frac{x_m}{1-x_T} = B \end{aligned} \tag{3.21}$$

Here h_{ms}, h_{ml} and h_{cl} are the cavity partition functions of methane in small cavities, methane in large cavities and carbon dioxide in large cavities respectively. The denominator in the second term can be expressed in terms of the mole fraction and one of the partition functions from equation 3.18 and 3.21

$$\begin{aligned} 1 + h_{ml} + h_{cl} &= (1 + Ah_{ms})C \\ C &= \left(1 + \frac{1}{\nu_l(1-x_T) - x_c}\right) \end{aligned} \tag{3.22}$$

Equation 3.21 now reduces to a second order equation on the form

$$\begin{aligned} a_1(h_{ms})^2 + a_2 h_{ms} + a_3 &= 0 \\ a_1 &= A(\nu_l + C\nu_s - BC) \\ a_2 &= C\nu_s + A\nu_l - BC(1+A) \\ a_3 &= -BC \end{aligned} \tag{3.23}$$

Solving this with respect to the cavity partition function h_{ms} , all partition functions are known and the chemical potentials in equation 3.16 and 3.19 can be calculated. The free energy density for the hydrate as a function of mole fractions are shown in figure 3.1.

The surface in figure 3.1 is restricted by the full filling of the cavities $x_c + x_m < 4/27$. However CO_2 only goes into the large cavities so for mole fractions of CH_4 less than the full filling of small cavities $x_m < 1/27$, the hydrate can never be fully occupied. This can be seen as the cut-off region to the right in the figure. Here the large cavities are fully occupied by the carbon dioxide and the small cavities are partly occupied by methane.

3.3 Fluid thermodynamics

The solubility of water in a fluid phase can be approximated by the Raoult's law, see **paper 5**. In the following we shall use x_w for the mole fraction of water in the aqueous phase and y_w in the fluid phase.

$$y_w = \frac{P^{sat}_w}{P} \tag{3.24}$$

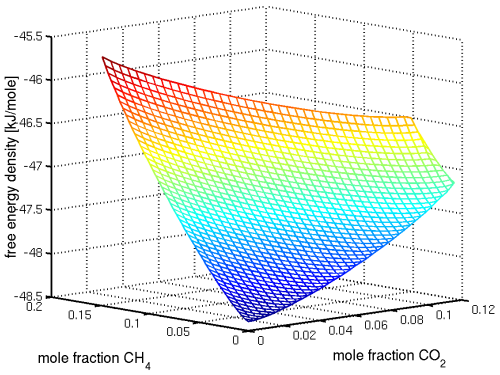

Figure 3.1: Free energy density (kJ/mole) as a function of the mole fractions of CH_4 and CO_2 at 1°C and 40 bars

The saturation pressure of water can be obtained from the empiric formula in the book by Reid Prausnitz and Sherwood [18]

$$\ln(P) = V_A - \frac{V_B}{T + V_C}, \tag{3.25}$$

with $V_A = 52.703$, $V_B = -3146.64$ and $V_C = -5.572$. We now consider the equilibrium of water in the fluid and aqueous phases, $\mu_w^F = \mu_w^{aq}$,

$$\mu_w^\infty + RT\ln(y_w) = \mu_w^p + RT\ln(x_w). \tag{3.26}$$

Here μ_w^∞ is the infinite dilution chemical potential of water in the fluid, μ_w^p is the chemical potential of pure water, which in [19] was estimated with a polynomial expansion in inverse temperature. Since $x_w \approx 1$ the last term in Eq. 3.26 can be neglected. We now have an expression for the infinite dilution chemical potential, and can use this to calculate the chemical potential of water in the fluid phase.

The chemical potential of the pure CO_2/CH_4 are calculated using the SRK equation of state [17]. The chemical potential in mixed fluid states are expressed as

$$\mu_i^F = \mu_i^{SRK,pure} + RT\ln(x_i) \tag{3.27}$$

where i is either CO_2 or CH_4.

3.4 Aqueous solutions

For the aqueous phase the solution of the solvents CO_2 and CH_4 in water is assumed to be independent of each other. In general they have the form

$$\mu_i = \mu_i^\infty + RT\ln(x_i\gamma_i) + \nu_i(P - P_0). \tag{3.28}$$

μ_i^∞ is the chemical potential of component i in water at infinite dilution, γ_i is the activity coefficient of component i in the aqueous solution in the asymmetric

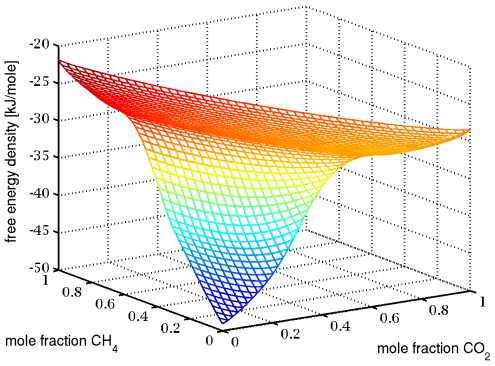

Figure 3.2: Free energy density (kJ/mole) as a function of the mole fractions of CH_4 and CO_2 at 1°C and 40 bars

convention (γ_i approaches unity in the limit of x vanishing). The chemical potentials at infinite dilution are found as functions of temperature by assuming the equilibrium between fluid and aqueous phases of CO_2/CH_4, $\mu_i^L = \mu_i^{aq}$, at low pressures where the solubility is very low and with thermodynamics of the fluids from the previous section and experimental values for the solubility. The activity coefficient is then fitted to solubility data at elevated pressures and mole fractions. In case of CO_2, data has been extracted from the empirical model by Diamond et. al. [20], with experimental data from Chapoy et. al. [21] and Lekvam et.al. [22] used for CH_4. The chemical potentials at infinite dilution were fitted to a polynomial in inverse temperature, the natural logarithm of the activity coefficient was fitted to a polynomial in mole fraction. Due to the very low solubility of CH_4 in water, the activity coefficient was approximated by unity.

$$\begin{aligned} \mu_i^\infty &= a_1 + \frac{a_2}{T} \\ \ln(\gamma_i^\infty) &= a_1 x_i + a_2 x_i^2 \end{aligned} \tag{3.29}$$

The coefficients a_1 and a_2 can be found in Table 1 in **paper 5**. For water, we have

$$\mu_w = \mu_w^p + RT \ln\left((1-x)\gamma_w\right) + \nu_w(P - P_0) \tag{3.30}$$

Where μ_w^p is pure water chemical potential. The activity coefficient in water, γ_w, can be obtained through the Gibbs-Duhem relation.

$$x d\ln(\gamma_c) + (1-x) d\ln(\gamma_w) = 0 \tag{3.31}$$

Where γ_c is the activity coefficient for CO_2, since the activity of CH_4 is approximated by unity it does not influence the activity of water either. Solving the Gibbs-Duhem equation with respect to the activity coefficient for water yields the following.

$$\ln(\gamma_w) = (2a_2 + a_1)\ln(1 - x_c) + a_2 x_c^2 + x_c(2a_2 + a_1) \tag{3.32}$$

In our phase field theory model, the aqueous and fluid phases are treated a single common phase. For this purpose a smooth free energy function has been constructed over the whole mole-fraction domain of both CO_2 and CH_4. In the water rich region the aqueous thermodynamics has been used and the fluid thermodynamics has been used in the fluid-rich region. In the non-physical region an artificial potential was utilized to ensure the splitting of the phases. The combined function are shown in Fig. 3.2. For two component simulations the free energy function along one of the pure component axes in Fig. 3.2 and 3.1 is used.

3.5 Hydrate equilibrium

Given the thermodynamic model outlined in the previous sections, the equilibrium conditions between phases can easily be computed. It is important to stress here that the thermodynamic functions have been derived with the aim of providing easily accessible expressions for the chemical potentials as a function of temperature, pressure and composition. Furthermore, the experimental data used to obtain model parameters pertained only to the aqueous/liquid equilibrium outside of the hydrate stability region. The hydrate equilibrium results presented were thus not adjusted to account for the experimental hydrate data. In Fig. 3.3 the dissociation pressure of CO_2 hydrate is shown as a function of temperature. For the temperature range shown in Fig. 3.3 CO_2 is in the gaseous phase, for higher temperatures we move into the region of liquid or fluid CO_2, where the SRK equation is not that accurate, and the equilibrium pressure is reproduced less accurate. Figure 3.4 shows the equilibrium mole fraction of CH_4 in the aqueous phase. The equilibrium data for CH_4 is in general not as accurate as the corresponding results for CO_2, this is partly due to a more simplified model for the CH_4 and less available experimental solubility data. Other equilibrium results can be found in **paper 5**.

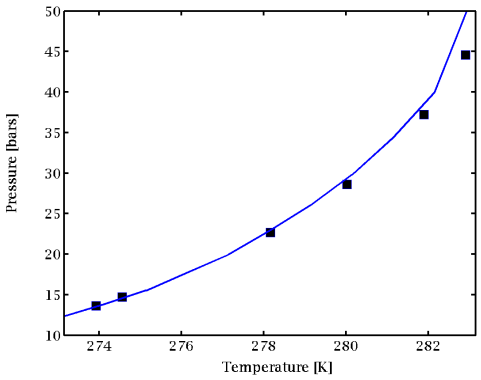

Figure 3.3: Dissociation pressure of CO_2 hydrate in the temperature range 0-10 °C. Calculated value (solid line) compared to experimental data by Wendland et. al. [23]

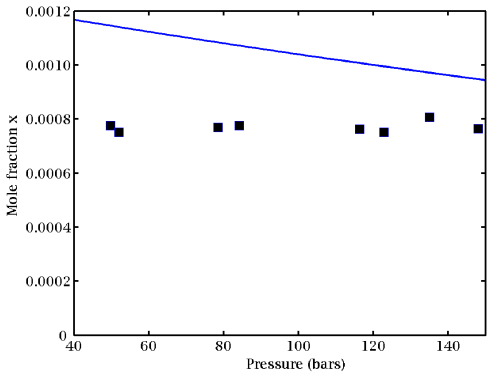

Figure 3.4: Mole fraction of CH_4 as a function of pressure. Model prediction (solid line) compared to experimental data by Yang et. al. [24] at 0°C

Chapter 4

Summary of the papers

The main portions of this thesis is devoted to the application of the phase field theory for simulation of hydrate phase transition kinetics. The computer code for the simulations in this work are modifications of the phase field code used by László Gránásy in the first application of the phase field theory on hydrates in a collaboration with Bjørn Kvamme [25]. A parameter sensitivity analysis was conducted for the homogeneous kinetics for CO_2 growing from aqueous solution. At least within the parameterization and approximations of the simulations it became clear that the most important parameter for this system was the liquid diffusivity. For this reason a conference on diffusion in liquids and solids was chosen as the appropriate place for presenting the first results of this thesis and **paper 1** was therefore submitted for this conference. The main focus of the paper was towards the liquid diffusion as a rate limiting factor. In this work the thermodynamics was similar to the one used in [25] with a correction in the expression for the partition function as a function of mole fraction. The square root behavior of the growth rate was presented, and the same growth rate was reproduced from considering the bulk diffusion in the liquid through the Fick's law and information of the concentration profile near the interface. The difference between growth and dissociation rates showed the appropriate and expected relationships to the initial supersaturated concentration in the solution and the equilibrium point between hydrate and the aqueous phase. The latter value was however not estimated with high accuracy within the approximate thermodynamic model applied in this paper. Furthermore, the paper also contains a discussion on the validity of the isothermal assumption in the simulations. It is argued that the released heat has little or no effect on the overall kinetics although we didn't rule out a potential effect of heat transport on the nucleation stage. Finally we also discuss the effects of anisotropic crystal growth on crystal morphology and the kinetic rates of growth. An oral presentation of the contents of the paper was given at the First International conference on Diffusion in Solids and Liquids at the University of Aveiro in Portugal on July 6th 2005. The paper was also selected by the conference organizers for publication in a special issue of the Journal of Phase Equilibria and Diffusion.

Paper 2 gives a more detailed presentation of the phase field simulations. The model is extended to also simulate the homogeneous growth of CH_4 hydrate from an aqueous solution. The thermodynamic model of CO_2 has also been altered by replacing the expression for the activity coefficient with a new

expression fitted to experimental solubility data. The old expression was a polynomial expansion in the logarithm of the mole fraction fitted to experimental data on the activity coefficient [25]. This expression did not fulfill the asymmetric convention in the limit as $x \to 0$, furthermore a simpler expression was desirable for the calculation of the activity coefficient of water. Growth rates for planar and circular geometries for both CO_2 and CH_4 were compared. The pressure dependency of the growth rate was also presented. Finally the anisotropic growth rate were compared to the isotropic growth rate. **Paper 2** was presented at a poster session at the 16th American Conference on Crystal Growth and Epitaxy held jointly with the 12th US Biennial Workshop on Organometallic Vapor Phase Epitaxy. A full journal paper will be published in a special edition of the Journal of Crystal Growth.

The main focus of **paper 3** is on the dissociation rates of CO_2 and CH_4 hydrate exposed towards pure water. The motivation for this study was the potential presence of a hydrate film during storage of CO_2 in cold reservoirs, and the dissociation rate of this film towards the contacting ground water on top. The motivation for the CH_4 hydrate dissociation study was the exposed hydrate reservoirs that continuously leak CH_4 to oceans due to the chemical potential difference of methane between the hydrate and the seawater. Models for these leakage rates enter as the primary source for chemical and biological ecosystems as well as transport towards the surface through ocean currents. Leakage of CH_4 to the atmosphere is an environmental concern. It is concluded that the dissociation rate of CO_2 hydrate is much larger than for CH_4 hydrate as expected from the differences in the solubility in water. The paper was presented at the International Conference of Computational Methods in Sciences and Engineering (ICCMSE-2005) by Bjørn Kvamme. An extended paper of the conference proceedings, **paper 4**, has been prepared and submitted for one of the journals associated with the conference. **Paper 4** includes the updated version of the thermodynamic model with corresponding simulation results. The paper also includes simulations of fluid CO_2 dissociating through a hydrate film as well as a discussion on dissociation of CH_4 coupled to the formation and escape of CH_4 bubbles.

In the process of developing a phase field theory for the three component system $H_2O/CO_2/CH_4$ full thermodynamic function in all phases has to be available as a function of the mole fractions, temperature and pressure. Such a model is presented in **paper 5** together with molecular dynamic results on the interface thermodynamics. This work represents the final model that has been gradually improved through **paper 1-4**. Thermodynamics for mixed hydrates are presented in this paper, and the thermodynamics for the aqueous CO_2 was improved to better reproduce experimental data. For fluid CO_2 the empirical equation of state model used in **paper 2** was replaced by an SRK equation of state due to problems with the temperature dependence in the computer code calculating the chemical potentials. It also became clear that the infinite dilution chemical potential was not compatible with the rest of the model. A new expression for this was obtained from fitting a new function to experimental data. The paper also contains comparisons of hydrate/aqueous equilibrium states with experimental work.

Paper 6 is an extensive presentation of the phase field theory applied to the nucleation and growth of CO_2 hydrate. The model parameters are related to atomistic simulation/experiments The growth rate of a single dendritic hy-

drate particle is extrapolated to experimental time scales and compared with experiments conducted at the same conditions. The discrepancy in growth rate are discussed and it is argued that the most probable source is a kinetic barrier due to complex molecular motions required for crystal growth.

Paper 7-9 treats another mean-field approach to the growth of hydrate. The model is a hybrid of cellular automata and Monte Carlo and has potential of being computationally more effective than the phase field theory. In **Paper 7** the model is presented and the growth of hydrate is studied at different supersaturations of aqueous CO_2, while **Paper 8** and **9** compares and discusses the model relative to the phase field approach.

Paper 10 was motivated by a project on aquifer storage of CO_2 in which the issue of hydrate sealing effects in cold reservoirs can assist in reducing the leakage flux of CO_2 from the reservoir. The paper was presented at the 7th International Conference Greenhouse Gas Control Technologies in Vancouver, Canada 2004. A general presentation of the phase field theory for the growth and dissociation of hydrate films is followed by corresponding simulation examples under conditions representative for storage of CO_2 in aquifers. Effects of local free energy gradients are also illustrated in this paper. Hydrate cores at the interface which have higher free energy than neighboring cores may eventually be consumed by supporting further growth of the cores with lower free energy.

Paper 11 is a review article giving a summary of our approaches to model hydrate phase transition kinetics, not including our later publications though. Simulation results are presented for the phase field theory and the cellular automata. Simulations on hydrate formation in a micro-pore structure and some preliminary results from the three component phase field theory are also presented.

Paper 12 is an extended abstract that has been submitted for the 8th International Conference on Greenhouse Gas Control Technologies, which is going to be held in Trondheim in June 2006. In this abstract we are relating thermodynamic properties and results from the PFT to the flux rates from a hydrate sealing layer.

Chapter 5

Further work

A three component phase field model

With the development of a three component thermodynamic model in paper 5, a natural next step is to fully implement this into a three component phase field theory. Work along these lines are already in progress in collaboration with László Gránásy. Some preliminary results has been presented in **paper 11**. The development of such a model will be central in learning more about the kinetics concerning the reformation from CH_4 to CO_2 hydrate.

Hydrodynamics

The current phase field model is assuming equal molar volume of all phases independent on composition. This is a fair approximation for the hydrate/aqueous system and also to a certain degree for fluid CO_2 at elevated pressures. For CH_4 and CO_2 in the gaseous phase it is not a good approximation and the effect of hydrodynamics is here expected to play a significant role for this system, depending on temperature, pressure and relative fractions of these components in a mixture. The inclusion of hydrodynamic effects into the phase field model can possibly give valuable insight into the process of nucleation and growth of hydrate. In particular relative to heterogeneous growth this effect is expected to represent a significant effect because a nearly impenetrable hydrate film is created at the interface between the two hydrate components. A phase field model with fluid flow can be found in [26].

Hydrates in pores

Hydrates in reservoirs are formed within the pores. Thermodynamic properties of the fluid and hydrate molecules at the mineral surface are therefore an issue of significance that depends upon the size of the pores and the specific mineral surfaces. The effect of surfaces on the liquid is frequently referred to as either water-wetting or oil-wetting (or non-polar wetting) depending on the interfacial tension between the water and mineral versus the corresponding property for oil and mineral. A water-wetting surface will reduce the chemical potential of pure water and thus implies a shifting of the hydrate stability point at the mineral interface. As a result an aqueous film is often present between the mineral

and the hydrate, depending on mineral type and thermodynamic conditions. This has been observed experimentally for silica pores and also observed in situ as in the Mallik project [27]. Other kinds of surfaces may lower the chemical potential of non-polar components such as the CO_2, causing adsorption of these components at the walls and thus making these adsorption sites more suitable for initial nucleation due to a high surface concentration of CO_2 relative to the solution concentration of CO_2. The effect of the presence of surfaces may be implemented into the phase field model through the inclusion of a new static field in the free energy functional. The properties at the surface interface can be obtained from molecular simulations. Work along these line is already in progress [28] and [29]. Typical sizes for pores in reservoirs range from a couple of micrometers and upwards. This system size can be within the reach for the phase field model to simulate. Knowledge of hydrate phase transitions within a single pore can then maybe be used to create models for hydrate formation and reformation in macroscopic reservoirs.

Phase field mobility

The actual concentration profile across the interface will in some regions reflect partially dissociated hydrate and on the other end supersaturated solution. In addition to this comes the effect of capillary waves and corresponding average concentrations. The approximation that concentration mobility is an weighted average of diffusivity coefficients represents at least an interpolation between two reasonable end points for the liquid and solid phases. The phase field mobility on the other hand, is a more complex issue with room for theoretical improvements. Hydrate formation from a dilute solution of guest molecules requires complex assembly of guest molecules and rearrangements of hydrogen bonded water molecules into a solid structure. The fundamental mechanisms of hydrate nucleation are not known but some information on dynamic aspects related to the phase transition can be achieved through molecular simulation studies of hydrate dissociation at conditions slightly outside equilibrium. Detailed samplings of the corresponding changes in rotational and translational modes of water and guest molecules might give insight into rate limiting terms and also partially quantification of corresponding mobilities for use in PFT simulations. Similar studies can also be conducted for hydrate growth by varying the supersaturation of guest molecules close to a hydrate core.

Numerical improvements

One of the problems with the phase field theory is that it takes a lot of time to run the simulations on computers. It is therefore important that the numerical routines are optimized for the best performance. By the introduction of a semi-implicit scheme in **paper 6**, an improved computer code was obtained. Another possible improvement will be to use some adaptive grid technique. Presently the simulations are done on a equidistant grid, which is not very efficient since the most important dynamics are taking place at the interface. Fewer grid points can be obtained by making the spatial resolution larger in the near bulk regions.

Hydrate sealing in reservoir simulations

In a collaboration with the research project "Safe long terms storage of CO_2 in aquifers", within Kvamme's research group, there is work in progress on the implementation of hydrate sealing in the thermal multi-phase 3D-transport reservoir simulator ATHENA. The idea is to implement a simple routine to determine the hydrate stability and then assume an instant formation of a hydrate layer, which is a reasonable assumption within a1 time step of the reservoir simulator. With knowledge of hydrate dissociation from phase field simulations the hydrate layer will be treated as a non-volume element with a lower permeability.

Hydrate growth and dissociation in saline water

The presence of salt ions in the water will lower the chemical potential of the aqueous water phase and thus shift the equilibrium conditions to higher equilibrium pressure for a fixed temperature or to a lower equilibrium temperature for a fixed pressure. The corresponding reduction in thermodynamic driving forces outside of equilibrium will have an impact on the rates of hydrate growth and dissociation. The salinity of groundwater in reservoirs will typically vary from close to zero up to seawater salinity, but can locally also be higher. And while seawater is dominated by sodium chloride some groundwater in reservoirs may locally contain higher concentrations of bivalent and trivalent ions of magnesium, calcium and iron. The effect is still expected to be most significant for hydrates directly exposed to the ocean at the sea floor. Instead of expanding the thermodynamic model by including the ions as separate components, they may be included by a correction factor to the chemical potential of the water with a fixed salinity. This approximation would be valid if the diffusion of salt ions is fast, which is probable since the diffusion coefficient of sodium chloride is one order of magnitude faster than the diffusion coefficient of CO_2 in water. Another issue relative to ions is the influence of products of CO_2 hydrolysis (HCO_3^-, CO_3^{2-}). The contents of HCO_3^- may be as high as 20%, but the chemical reaction is expected to be so fast that there will always be enough CO_2 available. This effect is negligble for the supersaturation of CO_2 in the aqueous phase in the $P-T$ region of interest [20].

Appendix A

Functionals and functional derivatives

Consider a function of several variables, $y_1, y_2, ...$, with partial derivatives $\partial F/\partial y_1$, $\partial F/\partial y_2, ...$ With a displacement $dy_1, dy_2, ...$ from the point $y_1^0, y_2^0, ...$, the function F will change according to

$$dF = \left.\frac{\partial F}{\partial y_1}\right|_{y^0} dy_1 + \left.\frac{\partial F}{\partial y_2}\right|_{y^0} dy_2 + ... \tag{A.1}$$

Let us divide an interval $[a, b]$ into N points with a distance ϵ apart so that $N\epsilon = b - a$ and with the $n^t h$ point at $x = x_n = a + n\epsilon$. A function $y(x)$ can be represented by its values on the N points, $y_n = y(x_n) = y(a + n\epsilon)$, which would converge towards the original $y(x)$ as $N \to \infty$ and $\epsilon \to 0$. A function of all the y_n can be defined, $F(y_n)$. In the limit $N \to \infty$, the function F becomes a function of the function $y(x)$. We then call F a *functional* of $y(x)$ written $F[y]$.

If we change the values of y_n the functional changes according to A.1. This can be rewritten as

$$dF = \sum_{n=1}^{N} \left.\frac{\partial F}{\partial y_n}\right|_{y^0} dy_n \tag{A.2}$$

. To find how this look in the $N \to \infty$ limit we recall the definition of an integral:

$$\int_a^b dx f(x) = \lim_{\epsilon \to 0} \sum_{n=1}^{N} \epsilon f(x_n). \tag{A.3}$$

If we then rewrite A.2 as

$$dF = \sum_{n=1}^{N} \epsilon \left(\frac{1}{\epsilon} \left.\frac{\partial F}{\partial y_n}\right|_{y^0} \right) dy_n, \tag{A.4}$$

taking the limit $\epsilon \to 0$, with $x = a + n\epsilon$, and introducing the notation $dy_n = \delta y(x)$, A.4 becomes

$$dF = \int_a^b dx \left.\frac{\delta F}{\delta y(x)}\right|_{y^0(x)} \delta y(x). \tag{A.5}$$

The $1/\epsilon$ has been absorbed into $\delta F/\delta y(x)$ and this can be taken as a definition of the *functional derivative* $\delta F/\delta y(x)$.

Consider the case where the functional F is an integral over an integrand L containing both y and $y' = dy/dx$.

$$F[y] = \int L(x, y, y')dx \tag{A.6}$$

A variation of $y(x)$ by some specific $\delta y(x)$ gives

$$F[y + \delta y] = \int L(x, y + \delta y, y' + \delta y')dx \tag{A.7}$$

where $\delta y' = d(\delta y)/dx$ is the derivative of the small variation $\delta y(x)$. Expanding to first order in δy and its derivative,

$$F[y + \delta y] \simeq \int \left(L(x, y, y') + \frac{\partial L(x, y, y')}{\partial y}\delta y + \frac{\partial L(x, y, y')}{\partial y'}\delta y' \right) dx \tag{A.8}$$

Integrating by parts gives

$$\begin{aligned} \int_a^b \frac{\partial L(x, y, y')}{\partial y'}\delta y' dx = \quad & \left[\frac{\partial L(x, y, y')}{\partial y'}\delta y(x) \right]_a^b \\ & - \int_a^b \frac{d}{dx}\left(\frac{\partial L(x, y, y')}{\partial y'} \right) \delta y(x)dx. \end{aligned} \tag{A.9}$$

The first term on the right hand side of A.9 is a boundary term and will vanish if the endpoints are not varied. Using A.9 in A.8 we obtain

$$dF = \int \left(\frac{\partial L(x, y, y')}{\partial y} - \frac{d}{dx}\frac{\partial L(x, y, y')}{\partial y'} \right) \delta y(x)dx. \tag{A.10}$$

We now compare with A.5 and conclude that

$$\frac{\delta F}{\delta y(x)} = \frac{\partial L}{\partial y} - \frac{d}{dx}\frac{\partial L}{\partial y'}. \tag{A.11}$$

The functional deriviative can be found from this equation whenever the functional is on the form of A.7, and for the general $R3$ case we have

$$\frac{\delta F}{\delta y} = \frac{\partial L}{\partial y} - \nabla \cdot \frac{\partial L}{\partial \bigtriangledown y}. \tag{A.12}$$

Bibliography

[1] E D Sloan. *Clathrate Hydrates of Natural Gas*. McGRAW-HILL BOOK COMPANY, 1998.

[2] Y F Makogon. *Hydrates of Hydrocarbons*. PENNWELL BOOKS, 1997.

[3] J H van der Waals and J C Platteeuw. Clathrate solutions. *Advances in Chemical Physics*, 2:1–57, 1959.

[4] O K Førrisdahl. *Computer simulations of natural gas hydrates:equilibrium, melting, inhibition and free energy calculations*. PhD thesis, 2002.

[5] V P Shpakov, B Kvamme, and Belosludov V R. Elastic moduli calculation and instability in structure i methane clathrate hydrate. *Chem. Phys. Lett.*, 282:107, 1998.

[6] M von Stackelberg and Müller H R. On the structure of gas hydrate. *J. Chem. Phys.*, 19:1319–1320, 1951.

[7] E D Sloan and F Fleyfel. A molecular mechanism for gas hydrate nucleation from ice. *AIChE J.*, 37:1281–1292, 1991.

[8] B Kvamme. A new theory for the kinetics of hydrate formation. In *2nd International Conference on Natural Gas Hydrates*, 1996.

[9] P Englezos, N Kalogerakis, P D Dholabhai, and P R Bishnoi. Kinetics of formation of methane and ethane gas hydrates. *Chemical Engineering Science*, 42:2647–2658, 1987.

[10] P Skovborg and P Rasmussen. A mass transport limited model for the growth of methane and ethane gas hydrates. *Chemical Engineering Science*, 49:1131–1143, 1994.

[11] A A Wheeler, W J Boettinger, and G B McFadden. Phase-field model for isothermal phase transitions in binary alloys. *Physical Review A*, 45(10):7424–7439, 1992.

[12] M Conti. Solidification of binary alloys: Thermal effects studied with the phase field. *Physical Review E*, 55(1):765–771, 1997.

[13] M Conti. Thermal and chemical diffusion in the rapid solidification of binary alloys. *Physical Review E*, 61(1):642–650, 2000.

[14] J A Warren and W J Boettinger. Prediction of dendritic growth and microsegregation patterns in a binary alloy using the phase-field method. *Acta Metall. Mater.*, 43:689–703, 1995.

[15] L Gránásy, T Börzsönyi, and T Pusztai. Nucleation and bulk crystallization in binary phase field theory. *Physical Review Letters*, 88(206105):1–4, 2002.

[16] R Radhakrishnan, A Demurov, H Herzog, and B L Trout. A consistent and verifiable macroscopic model for the dissolution of liquid co_2 in water under hydrate forming conditions. *Energy Conversion and Management*, 44:771–780, 2003.

[17] G Soave. Equilibrium constants for a modified redlich-kwong equation of state. *Chem. Eng. Sci.*, 27:1197–1203, 1972.

[18] R C Reid, J M Prausnitz, and T K Sherwood. *The Properties of Gases and Liquids*. McGRAW-HILL BOOK COMPANY, 1977.

[19] B Kvamme and H Tanaka. Thermodynamic stability of hydrates for ethane, ethylene and carbon dioxide. *J. Chem. Phys.*, 99:7114–7119, 1995.

[20] L W Diamond and N N Akinfiev. Solubility of co_2 in water from -1.5 to 100 °c and from 0.1 to 100 mpa: evaluation of literature data and thermodynamic modeling. *Fluid Phase Equlibria*, 208:265–290, 2003.

[21] A Chapoy, A H Mohammaid, D Richon, and B Tohidi. Gas solubility measurment and modeling for methane-water and methane-ethane-*n*-buthane-water systems at low temperature conditions. *Fluid Phase Equlibria*, 220:113–121, 2004.

[22] Dissolution of methane in water at low temperatures and intermediate pressures. Gas solubility measurment and modeling for methane-water and methane-ethane-*n*-buthane-water systems at low temperature conditions. *Fluid Phase Equlibria*, 131:297–309, 1996.

[23] M Wendland, H Hasse, and G Maurer. Experimental pressure-temperature data on three- and four-phase equilibria of fluid, hydrate, and ice phases in the system carbon dioxide-water. *J. Chem. Eng. Data*, 44:901–906, 1999.

[24] S O Yang, S H Cho, H Lee, and C S Lee. Measurement and prediction of phase equilibria for water + methane in hydrate forming conditions. *Fluid Phase Equilibria*, 185:53–63, 2001.

[25] B Kvamme, A Graue, E Aspenes, T Kuznetsova, L Gránásy, G Tóth, T Pusztai, and G Tegze. Kinetics of solid hydrate formation by carbon dioxide: Phase field theory of hydrate nucleation and magnetic resonance imaging. *Physical chemistry chemical physics*, 6(9), 2003.

[26] G Tegze, Pusztai T, and L Gránásy. Phase field simulation of liquid phase separation with fluid flow. *Mater. Sci. Eng. A*, 413-414:418–422, 2005.

[27] K Techmer, T Heinrich, and W F Kuhs. Cryo-electron microscopic studies on the structures and compositions of mallik gas-hydrate-bearing samples. *Geological Survey of Canada Bulletin*, 585, 2005.

[28] B Kvamme, T Kuznetsova, and D Uppstad. In *Proceedings from the International Conference of Computational Methods in Sciences and Engineering*, 2005.

[29] B Kvamme and T Kuznetsova. In *Proceedings from the International Conference of Computational Methods in Sciences and Engineering*, 2005.